openheart

CMR feature tracking in patients with dilated cardiomyopathy: patterns of myocardial strain and focal fibrosis

Céleste Chevalier ,[1] Katja Kremer,[2] Ersin Cavus,[1,3] Jan Schneider,[1] Charlotte Jahnke,[1] Gerhard Schön ,[4] Ulf K Radunski,[5] Enver Tahir,[6] Gerhard Adam,[6] Gunnar Lund,[6] Paulus Kirchhof,[1,3] Stefan Blankenberg,[1,3] Kai Muellerleile[1,3]

► Additional supplemental material is published online only. To view, please visit the journal online (http://dx.doi.org/10.1136/openhrt-2022-002013).

To cite: Chevalier C, Kremer K, Cavus E, *et al*. CMR feature tracking in patients with dilated cardiomyopathy: patterns of myocardial strain and focal fibrosis. *Open Heart* 2022;**9**:e002013. doi:10.1136/openhrt-2022-002013

Received 7 March 2022
Accepted 12 September 2022

For numbered affiliations see end of article.

Correspondence to
Dr Céleste Chevalier; c.chevalier@uke.de

ABSTRACT

Background There is a paucity of data on cardiovascular magnetic resonance feature tracking (CMR-FT) in patients with dilated cardiomyopathy (DCM). We aimed at describing global and segmental myocardial strain patterns and a potential association with the presence of focal myocardial scarring in DCM patients by CMR-FT.

Methods Thirty-nine patients with DCM and reduced left ventricular (LV) ejection fraction (mean 21±8%) underwent CMR including standard cine steady-state free precession (SSFP) sequences and late gadolinium enhancement (LGE). We measured global LV longitudinal as well as global and segmental circumferential and radial strain. The presence of focal myocardial fibrosis was assessed on LGE images.

Results Nineteen patients had focal myocardial fibrosis on LGE images with the highest prevalence in the basal septal segments II and III, which were affected in 12 (63%) and 13 (68%) patients. Furthermore, there was a significantly lower average short-axis LV radial strain (LV_{SAX}-RS) in these segments (4.89 (−1.55 to 11.34) %) compared with the average of the other myocardial segments (21.20 (17.36 to 25.05)%; p<0.001) after adjusting for LGE and left-bundle branch block (LBBB). In general, LV segments with LGE had lower model-based mean LV_{SAX}-RS values (17.65 (10.37 to 24.93) %) compared with those without LGE (19.40 (15.43 to 23.37) %), but this effect was not significant after adjusting for the presence of LBBB (p=0.630).

Conclusion Our findings revealed a coincidence of impaired radial strain and focal myocardial fibrosis in the basal septal LV myocardial segments of patients with DCM. Regardless of this pattern, we did not find a general, significant effect of myocardial fibrosis on strain in our cohort. Future studies are required to assess the potential prognostic implications of myocardial strain patterns in addition to the assessment of myocardial fibrosis in patients with DCM.

WHAT IS ALREADY KNOWN ON THIS TOPIC

⇒ There is a need for a more detailed characterisation of patients with dilated cardiomyopathy (DCM) beyond traditional measurements of left ventricular ejection fraction (LVEF). Strain imaging by cardiovascular magnetic resonance feature tracking (CMR-FT) is an emerging method for an advanced assessment of myocardial function. However, there is currently a paucity of data on strain patterns and potential associations with myocardial fibrosis in DCM patients. Therefore, we performed CMR-FT and myocardial fibrosis imaging by CMR in a prospectively recruited cohort of DCM patients with severely reduced LVEF.

WHAT THIS STUDY ADDS

⇒ We observed a pattern with significantly lower radial strain values in the basal septal segments compared with the other myocardial segments in our cohort of DCM patients. These basal septal segments also had the highest presence of focal myocardial fibrosis. However, our analyses did not show a significant effect of the presence of focal myocardial fibrosis on radial strain after adjusting for left-bundle branch block.

HOW THIS STUDY MIGHT AFFECT RESEARCH, PRACTICE OR POLICY

⇒ Our findings represent a first step towards a better understanding of the interactions between functional strain characteristics and focal myocardial fibrosis in DCM. Our findings encourage future studies to assess the potential incremental prognostic implications of myocardial strain patterns in comparison to traditional cardiac imaging.

INTRODUCTION

Dilated cardiomyopathy (DCM) is a common cause of heart failure.[1] Patients show diverse aetiologies and symptoms,[2 3] but are overall affected by substantial morbidity and mortality.[4] In the diagnostic process, cardiovascular MRI (CMR) can be particularly useful as it accurately analyses cardiac anatomy and function, and differentiates underlying pathologies, for example, by identifying myocardial scarring by late gadolinium enhancement (LGE) and/or T1 mapping CMR.[5 6] In addition to conventional imaging, CMR strain imaging is an emerging method

in the assessment of myocardial function in patients with DCM beyond traditional volumetric left ventricular ejection fraction (LVEF) calculation.[7] Recent studies reported impaired global left ventricular (LV) strain in DCM,[8 9] but also a potential association of strain-derived parameters with cardiac outcome.[8 10] A particularly feasible method of strain imaging is CMR feature tracking (CMR-FT). This method uses standard cine CMR images and does not require the acquisition of additional sequences.[7 11] Yet, the literature on the topic of CMR-FT in DCM is still scarce. Therefore, this study aimed at assessing global and segmental myocardial strain patterns via CMR-FT and potential associations with myocardial scarring/fibrosis in DCM patients.

METHODS

Study population

This prospective study included 39 patients with DCM who underwent CMR between January 2017 and February 2019. DCM was defined by the presence of LV dilatation and a reduced LVEF <40 % in the absence of significant coronary artery disease or evidence for acute myocardial inflammation as recommended.[3 12] Exclusion criteria included renal insufficiency with a glomerular filtration rate (eGFR) <30 mL/min/1.73 m^2 and general contraindications to CMR. Laboratory analysis included cardiac biomarker N-terminal prohormone of the brain natriuretic peptide (NT-proBNP) ± 14 days before/after CMR. All patients received a standard transthoracic echocardiography±14 days before/after CMR.

Cardiovascular MRI protocol

Twenty-eight patients were scanned on a 1.5-T scanner (Achieva, Philips Medical Systems, Best, The Netherlands) and 11 patients were scanned on a 3.0-T scanner (Ingenia, Philips Medical Systems, Best, The Netherlands). The CMR imaging protocol included cine imaging, native T1 mapping and LGE imaging. Cine images were acquired in long-axis (four-chamber, two-chamber and three-chamber view) and a short-axis stack covering the LV with standard retrospectively gated steady-state free precession (SSFP) sequences. Typical imaging parameter were as follows: 1.5 T: voxel size 1.36×1.36×6 mm^3, echo time=1.57 ms, time to repetition=3.14 ms, flip angle=60°, parallel acquisition technique=SENSE; 3.0 T: voxel size 1.36×1.36×6 mm^3, echo time=1.39 ms, time to repetition=2.79 ms, flip angle=45°, parallel acquisition technique=SENSE. A typical temporal resolution was 26 ms. LGE images were acquired using a standard phase-sensitive inversion recovery (PSIR) sequence at least 10 min after bolus injection of 0.2 mmol/kg contrast agent (gadoterate meglumine (Dotarem, Guerbet, Sulzbach, Germany) in a stack of short-axis slices and in three long-axis orientations corresponding to the views used for Cine imaging. Typical imaging parameters were as follows: 1.5 T: voxel size 1.22×1.22×8 mm^3, echo time=2.40 ms, time to repetition=4.98 ms, flip angle=15°; 3.0 T: voxel size 0.99×0.99×8 mm^3, echo time=3.00 ms, time to repetition=6.07 ms, flip angle=25°. Native T1 mapping was performed using a 5s(3s)3s modified look-locker inversion recovery (MOLLI) sequence on three short-axes slices (apical, mid-ventricular and basal).

CMR analysis

Two trained, blinded observers independently analysed the CMR data. Commercially available postprocessing software (Medis Suite MR, QMass, Medis Medical Imaging, Leiden, The Netherlands) was used to assess volumes and function of all cardiac chambers. LV and right ventricular (RV) volumes as well as LVEF and LV mass were evaluated from short-axis cine images. Left atrial (LA) and right atrial (RA) volumes were quantified using the biplane area-length method as recommended.[6] CMR parameters were indexed to the calculated body surface area. Values were interpreted in comparison to recently published reference values.[13] Native myocardial T1 values were obtained in a septal region of interest as recommended.[5] The presence of LGE was assessed qualitatively and quantitatively by using the commercially available and established software cvi42 (Circle Cardiovascular Imaging, Calgary, Alberta, Canada) and by applying the SD-based method (3-SD) as recommended.[14] LGE was assigned to myocardial segments according to the American Heart Association (AHA) segment model.[15]

CMR-FT analysis was performed using the QStrain application of Medis Suite MR (Medis Suite MR, QStrain, Medis Medical Imaging, Leiden, The Netherlands) as previously described.[16] The endocardial and epicardial contours were manually drawn in QMass and then copied to QStrain to ensure most accurate tracing points. Trabeculae and papillary muscles were excluded from myocardial mass. In line with current recommendations[11 17] global LV strain was assessed from endocardial and epicardial contours as global longitudinal strain (GLS) in long-axis cine images and as global radial strain (GRS) and global circumferential strain (GCS) in short-axis cine images. Segmental LV strain analysis included the evaluation of segmental circumferential and radial strain from short-axis cine images. We divided the LV myocardium into 16 segments for each patient according to the AHA segment model.[15] Negative values for longitudinal strain represent longitudinal shortening from base to apex while negative values for circumferential strain represent shortening along the circular outline in short axis. Positive values for radial strain stand for LV wall contraction.[17] LA/RA maximum was set at LV end-systole and LA/RA minimum was defined at LV end diastole.

Statistical analysis

Statistical analyses were performed using SPSS Statistics (V.25.0, Statistical Package for the Social Sciences, International Business Machines, Inc., Armonk, New York, USA) and R V.4.2.0[18] including R-package lmerTest V.3.1.3[19] and R-package effects V.4.2.2.[20] Histograms were evaluated for deviations of the normality assumption. Accordingly, data

Table 1 Clinical characteristics

Clinical parameters (unit)	Mean±SD/number (percentage)
Age (years)	52±15
Sex (male)	31 (79.5%)
Heart rate (beats/min)	80±12 (n missing=4)
NYHA Class	(10.3%) (n missing=4)
I	3 (7.7%)
II	12 (30.8%)
III	16 (41.0%)
IV	4 (10.3%)
Atrial fibrillation	
Yes	10 (25.6%)
No	29 (74.4%)
Intraventricular block	
Yes	9 (23.1%)
No	33 (76.9%)
LBBB	4 (10.3%)
Endomyocardial biopsy	10 (25.6%)
NT-proBNP (pg/mL)	4853±4990 (n missing=3)
GFR (mL/min)	78±22 (n missing=6)
QRS duration (ms)	111±23 (n missing=1)
LVEF by echocardiography (%)	24±8
TAPSE (mm)	18±5

Values for continuous data are given as mean and SD. Values for categorical data are given as counts and percentage of total column number.
GFR, glomerular filtration rate; LBBB, left bundle branch block; LVEF, left ventricular ejection fraction; NT-proBNP, N-terminal prohormone of the brain natriuretic peptide; NYHA, New York Heart Association; TAPSE, Tricuspid Annular Plane Systolic Excursion.

Table 2 CMR characteristics

General CMR parameters (unit)	Mean±SD/number (percentage)
LVEF (%)	21±8 (n missing=1)
LVEDVi (mL/m^2)	163.31±33.61 (n missing=1)
LVESVi (mL/m^2)	129.69±35.26 (n missing=1)
LV Mass Index (g/m^2)	53.70±13.43 (n missing=1)
RVEF (%)	44±15.78 (n missing=1)
RVEDVi (mL/m^2)	55.79±24.38
RVESVi (mL/m^2)	33.20±19.33
LAVi (mL/m^2)	59.82±24.74 (n missing=3)
RAVi (mL/m^2)	40.84±20.90
LGE	
Yes	19 (48.7%)
No	16 (41.0%)
na	4 (10.3%)
LGE mass (g)	6.76 (± 6.18)
LGE mass (%)	7.83 (± 6.54)
T1 native midventricular (ms)	
1.5 T (n=28)	1088±55 (n missing=1)
3 T (n=11)	1213±134
T1 native basal (ms)	
1.5 T (n=28)	1101±38 (n missing=1)
3 T (n=11)	1265±127
Strain parameters	Mean±SD
Strain parameters global (%)	
LV_{LAX}-GLS	−8.20±3.12
LV_{SAX}-GCS	−6.62±3.03
LV_{SAX}-GRS	25.44±14.60

Values for continuous data are given as mean and SD. Values for categorical data are given as counts and percentage of total column number.
GCS, global circumferential strain; GLS, global longitudinal strain; GRS, global radial strain; LAVi, left atrial volume index; LGE, late gadolinium enhancement; LVEDVi, left ventricular end-diastolic volume index; LVEF, left ventricular ejection fraction; LVESVi, left ventricular end-systolic volume index; RAVi, right atrial volume index; RVEDVi, right ventricular end-diastolic volume index; RVEF, right ventricular ejection fraction; RVESVi, right ventricular end-systolic volume index.

for continuous variables are presented as mean and SD or median and IQR (Q1 and Q3). Categorical variables are presented as numbers and percentage. Interobserver and intraobserver reproducibility was assessed using Bland-Altman analysis.[21] Analyses/comparisons of strain values between groups of patients were made using linear regression analysis. Analyses/comparisons of strain values between myocardial segments were made by applying random intercept models. All models were adjusted for the presence of left bundle branch block (LBBB). Spearman's correlation coefficient (r, rho) was used to assess correlations between global strain values and native T1. Statistical significance was defined as $p<0.05$.

RESULTS

Clinical and general CMR characteristics of DCM patients

Detailed clinical characteristics of the study population are provided in table 1 and detailed CMR characteristics are listed in table 2. Analysis of LV function and volumes was not possible in one patient due to inadequate quality of short-axis cine images. Nineteen (49%) patients had focal myocardial LGE.

Interobserver and intraobserver agreement of strain measurements

Mean interobserver differences (± SD) for global parameters were 0.09±1.82 for LV_{LAX}-GLS, −0.73±2.14 for LV_{SAX}-GCS and −2.30±21.01 for LV_{SAX}-GRS, respectively. For segmental strain parameters, mean interobserver differences (± SD) were −0.21±9.03 for CS and −0.32±39.99 for RS. Mean intraobserver differences (± SD) were −0.20±1.31 for LV_{LAX}-GLS, −0.43±1.49 for

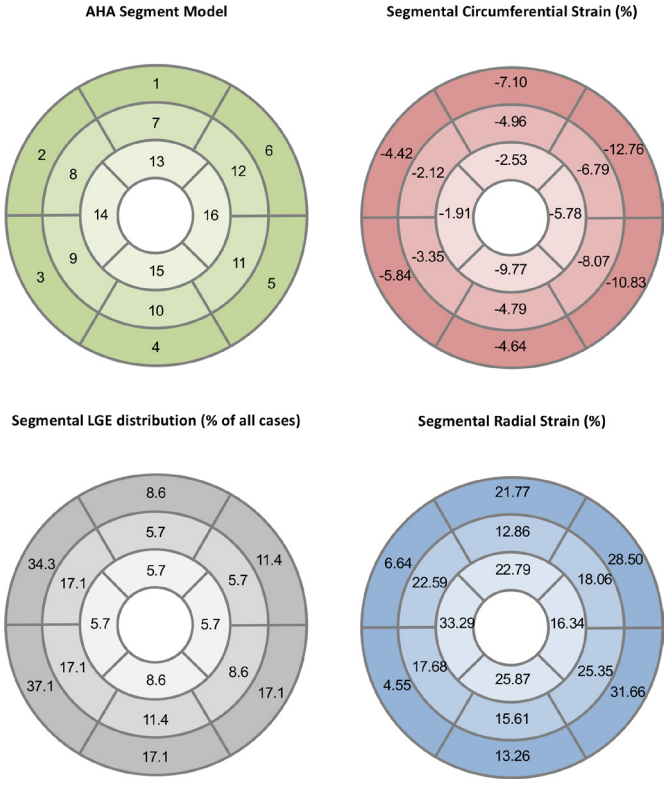

Figure 1 Late gadolinium enhancement (LGE) distribution and segmental strain values. LGE distribution and segmental LV_{SAX}-GCS and LV_{SAX}-GRS in dilated cardiomyopathy (DCM) patients in a bulls-eye plot according to the American Heart Association (AHA) segment model.[15] LGE frequency per segment is given as % of all LGE positive cases. Segmental strain values are provided as mean values.

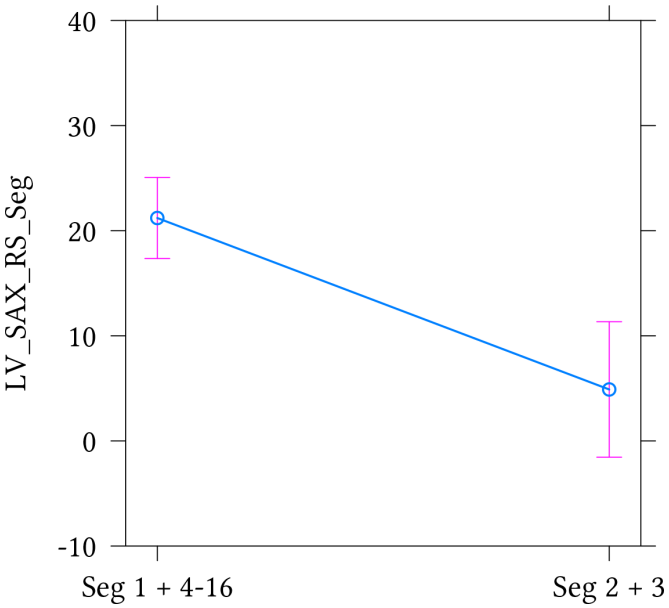

Figure 2 Mean model-based LV_{SAX}-RS value of the average of the basal septal segments II and III and the average of the other myocardial segments. Group differences were calculated by applying a random intercept model. Mean LV_{SAX}-RS value segments II+III: 4.89 (−1.55 to 11.34) %, mean LV_{SAX}-RS value segments I+IV – XVI: 21.20 (17.36 to 25.05) %, p<0.001.

LV_{SAX}-GCS and 0.69±11.26 for LV_{SAX}-GRS, respectively. For segmental RS and CS, mean intraobserver differences (± SD) were −0.39±4.56 for CS and 2.93±26.04 for RS.

Global myocardial strain

Mean LV_{LAX}-GLS was −8.20±3.12 %, mean LV_{SAX}-GCS was −6.62±3.03% and mean LV_{SAX}-GRS was 25.44±14.60% (table 2). There was no significant correlation of native myocardial T1 values in the basal septal myocardium at 1.5 T or 3 T with global strain parameters (1.5 T: LV_{LAX}-GLS r=0.23, p=0.243; LV_{SAX}-GCS r=0.07, p=0.739; or LV_{SAX}-GRS r=−0.17, p=0.415; 3 T: LV_{LAX}-GLS r=−0.56, p=0.090; LV_{SAX}-GCS r=−0.07, p=0.865; or LV_{SAX}-GRS r=0.17, p=0.668). Native mid-ventricular myocardial T1 values at 1.5 T did not show a significant correlation with LV_{LAX}-GLS or LV_{SAX}-GCS but correlated significantly with LV_{SAX}-GRS (r=−0.42, p=0.035).

Regional distribution of LV strain

Figure 1 demonstrates the regional distribution of LV_{SAX}-RS and LV_{SAX}-CS. Impairment of LV_{SAX}-RS was pronounced in the basal septal segments II and III (figure 1, online supplemental table 1), whereas the adjacent mid-ventricular septal segments, basal anterior and inferior as well as basal lateral segments had preserved mean LV_{SAX}-RS values (figure 1). According to the applied model, there was a significantly lower mean LV_{SAX}-RS value of the average of the basal septal segments II and III (4.89 (−1.55 to 11.34) %) compared with the average of the other myocardial segments (21.20 (17.36 to 25.05)%; p<0.001) (figure 2) after adjusting for focal myocardial fibrosis and left-bundle branch block (LBBB). Mean model-based LV_{SAX}-CS values were overall higher in the lateral myocardial segments. The highest values were found in the basal lateral segments V (−10.83 (−13.87, −7.34) %) and VI (−12.76 (−16.37, −8.92) %) (figure 1, online supplemental table 1).

Focal myocardial fibrosis

General and global LV characteristics

Four patients had to be excluded from this analysis due to missing or inadequate quality of LGE images. Nineteen of the remaining 35 patients had focal myocardial fibrosis on LGE images. Focal myocardial fibrosis was most frequently located in the basal septal segments II (n=12, 63%) and III (n=13, 68%) (figure 1). Mean LGE extent of LGE-positive patients was 6.76 (± 6.18) g or 7.83 (± 6.54) % of total myocardial mass. The predominant pattern were 'mid-wall' linear scarring (n=7, 36%) and focal scarring at RV insertion points (n=6, 32%). There were no significant differences in any demographic and general CMR-derived parameters between patients with and without focal myocardial scar (table 3). According to the applied model adjusted for LBBB, the presence of any LGE did not have a significant effect on global strain values (LV_{LAX}-GLS: p=0.625; LV_{SAX}-GCS: p=0.802;

Table 3 Clinical, general CMR and global strain parameters of DCM patients with (+) and without (–) LGE

	LGE + (n=19)	LGE – (n=16)	P value
Clinical parameters (unit)	Mean±SD/number (percentage)	Mean±SD/number (percentage)	
Age at MRI (years)	52±17	49±12	0.52[2]
Sex (male)	15 (78.9%)	13 (81.3%)	1.00[1]
Heart rate (beats/min)	77±14 (n missing=2)	84±9 (n missing=2)	0.13[2]
NYHA Class			0.16[1]
0	3 (15.8%)	1 (6.3%)	
I	1 (5.3%)	2 (12.5%)	
II	2 (10.5%)	7 (43.8%)	
III	10 (52.6%)	5 (31.3%)	
IV	3 (15.8%)	1 (6.3%)	
Atrial fibrillation			1.00[1]
Yes	4 (21.1%)	4 (25.0%)	
No	15 (78.9%)	12 (75.0%)	
Intraventricular block			0.56[1]
Yes	5 (26.3%)	3 (18.8%)	
No	14 (73.7%)	13 (81.2%)	
NT-proBNP (pg/mL)	6142±6139 (n missing=2)	3524±3328	0.14[2]
GFR (mL/min)	80±19 (n missing=2)	86±18 (n missing=4)	0.35[2]
QRS duration (ms)	110±23 (n missing=1)	113±25	0.72[2]
EF echocardiography (%)	22±8	25±8	0.38[2]
TAPSE (mm)	17±6 (n missing=2)	18±4 (n missing=1)	0.79[2]
General CMR parameters (unit)	Mean±SD	Mean±SD	
LVEF (%)	21±8 (n missing=1)	22±8	0.99[2]
LVEDVi (mL/m^2)	165.74±38.62 (n missing=1)	162.68±28.03	0.80[2]
LVESVi (mL/m^2)	131.88±41.96 (n missing=1)	128.14±28.12	0.77[2]
LV Mass Index (g/m^2)	54.11±16.67 (n missing=1)	54.51±10.34	0.94[2]
RVEF (%)	43±16 (n missing=1)	46.13±17.18	0.64[2]
RVEDVi (mL/m^2)	56.10±23.52	54.54±24.18	0.85[2]
RVESVi (mL/m^2)	33.12±18.01	32.24±20.72	0.90[2]
LAVi (mL/m^2)	63.76±18.96 (n missing=2)	55.91±26.31 (n missing=1)	0.34[2]
RAVi (mL/m^2)	41.35±20.17	40.44±22.50	0.90[2]
T1 native (ms) midventricular			
1.5 T (n=26)	n=16	n=10	0.87[2]
	1086±66	1090±36	
3 T (n=8)	n=3	n=5	0.08[t2]
	1335±20	1154±143	
T1 native (ms) basal			
1.5 T (n=26)	n=16	n=10	0.65[2]
	1098±43	1105±31	
3 T (n=8)	n=3	n=5	0.08[t2]
	1368±32	1211±153	
Strain parameters global (%)	Mean±SD	Mean±SD	
LV_{LAX}-GLS	–8.55±3.48	–7.89±2.78	0.55[2]
LV_{SAX}-GCS	–6.84±3.21 (n missing=1)	–6.48±3.15 (n missing=1)	0.75[2]
LV_{SAX}-GRS	27.62±13.64 (n missing=1)	25.32±15.54) (n missing=1)	0.65[2]

Values for continuous data are given as mean and SD. Values for categorical data are given as counts and percentage of total column number. Group differences were calculated with: [1]Fisher's exact test for categorical data or. [2]t-test for independent samples for continuous data. Statistically significant results: t, p ≤ 0.1; *, p ≤ 0.05; ** p, ≤ 0.01; *** p, ≤ 0.001. Note: four patients had to be excluded from analysis due to missing (n = 3) or inadequate quality of PSIR sequences (n = 1). CMR, cardiovascular MRI; GCS, global circumferential strain; GFR, glomerular filtration rate; GLS, global longitudinal strain; GRS, global radial strain; LGE, late gadolinium enhancement; LV, left ventricular; NT-proBNP, N-terminal prohormone of the brain natriuretic peptide; PSIR, phase-sensitive inversion recovery.

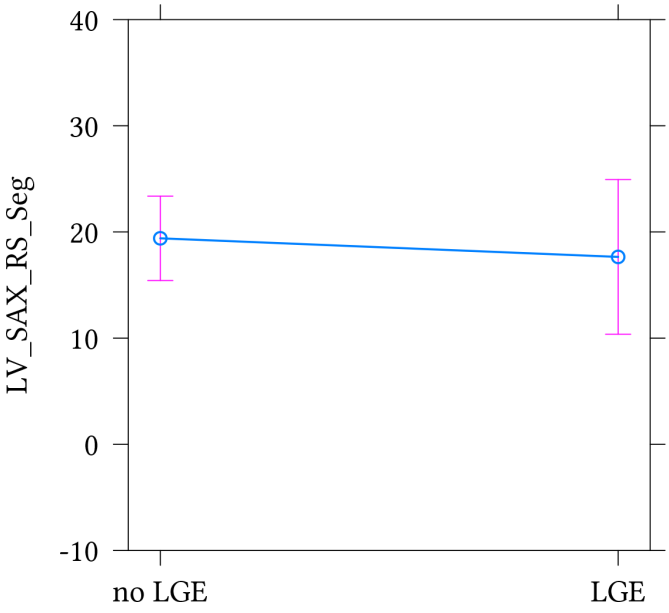

Figure 3 Mean model-based segmental LV_{SAX}-RS values of myocardial segments with and without late gadolinium enhancement (LGE). Group differences were calculated by applying a random intercept model. Mean LV_{SAX}-RS in myocardial segments with LGE: 17.65 (10.37 to 24.93) %, mean LV_{SAX}-RS in myocardial segments without LGE: (19.40 (15.43 to 23.37) %), p=0.630.

LV_{SAX}-GRS p=0.722). There was also no significant effect of mid-wall linear LGE on global strain values compared with non-mid-wall LGE (LV_{LAX}-GLS: p=0.603; LV_{SAX}-GCS: p=0.826; LV_{SAX}-GRS p=0.744) or to no LGE (LV_{LAX}-GLS: p=0.868; LV_{SAX}-GCS: p=0.510; LV_{SAX}-GRS p=0.801). There was a mean basal myocardial T1 at 1.5 T of 1101±38 ms and mean myocardial T1 at 3 T of 1265±127 ms. Mean mid-ventricular myocardial T1 was 1088±55 ms at 1.5 T and 1213±134 ms at 3.0 T (table 2).

Regional characteristics

There were 76 (13.6 %) myocardial segments with and 484 (86.4 %) myocardial segments without focal myocardial scar. According to the applied model, myocardial segments with LGE had a lower mean LV_{SAX}-RS (17.65 (10.37 to 24.93) %) than myocardial segments without LGE (19.40 (15.43 to 23.37) %) (figure 3). The presence of LGE was associated with a mean decrease in LV_{SAX}-RS of −1.75% (CI −8.81 to 5.53 %). However, this effect was not significant after adjusting for LBBB (p=0.630). An analysis focused on the basal septal segments II and III showed a model-based mean LV_{SAX}-RS of 8.89 (1.98 to 15.80)% in segments II and III with LGE compared with a model-based mean LV_{SAX}-RS of 4.04 (−0.96 to 9.05)% in segments II and III without LGE. There was no significant effect of the presence of LGE on LV_{SAX}-RS values (p=0.253). Furthermore, there was no significant association of mean LV_{SAX}-CS values and LGE (p=0.661). Mean LV_{SAX}-CS and LV_{SAX}-RS values for each segment in comparison to LGE distribution are provided in figure 1.

DISCUSSION

In this study, we describe global and segmental myocardial strain patterns by CMR-FT in a population of DCM patients with severely reduced LVEF. Briefly, we observed a coincidence of impaired radial strain and focal myocardial fibrosis in the basal septal LV myocardial segments in these patients. However, we did not find a general, significant effect of focal myocardial fibrosis on regional or global strain in our cohort.

Global myocardial strain

Overall, DCM patients had impaired LV_{LAX}-GLS, LV_{SAX}-GCS and LV_{SAX}-GRS (table 2) compared with reference values in healthy individuals using the same method,[16] corresponding to a severely reduced LVEF with a mean of 21%±8% (table 1). Reference values for global strain measurements from a recent publication of our group using an identical approach were as follows: median LV_{LAX}-GLS: −23.5 (−25.5, −22.0) %, median LV_{SAX}-GCS: −23.3 (−27.9, −21.1) %, median LV_{SAX}-GRS: 119.6 (91.3, 143.7) %.[16] While EF mostly depends on radial myocardial function, strain also reflects longitudinal and circumferential function.[22] In DCM, myocardial damage is not limited to one myocardial layer, but involves all layers.[23] An evaluation of strain characteristics independent from other functional parameters such as EF therefore could offer additional value. One study, for example, reported LV GLS as independent predictor of mortality in ischaemic and non-ischaemic DCM, incremental to EF.[10] Another study in DCM patients showed that reduced GLS in CMR-FT was an independent prognostic marker for a composite cardiac endpoint of cardiac death, heart transplantation, and aborted SCD and was a superior risk predictor compared with NYHA and EF.[24] A recent CMR study involving 350 DCM patients could show a prognostic value of other global LV strain parameters besides GLS as well.[25] Thus, strain assessment via CMR-FT could improve risk stratification for DCM patients in addition to other parameters.[24 25]

Analysis adjusted for the presence of LBBB did not reveal a significant effect of LGE on global strain values (table 3). LGE has been described in 12%–35% of DCM patients, most frequently as 'mid-wall' linear LGE.[26] LGE has proven to be an independent prognostic marker for adverse cardiac events including all-cause mortality, future hospitalisation and sudden cardiac death.[27–30] To the best of our knowledge, only two studies have investigated the relationship of fibrosis and strain via CMR-FT in DCM so far. Csecs *et al* found no significant difference in global LV strain parameters between LGE-positive and LGE-negative patients, similar to our results. The analysis of patients with septal fibrosis, however, revealed more severely reduced GCS and GRS, but not GLS, compared with patients without septal scarring.[31] Taylor *et al* found that the presence of mid-wall fibrosis significantly impaired GCS, while GLS and GRS were not affected.[32] We did not observe a significant effect of the presence of mid-wall linear LGE on LV_{SAX}-GRS values compared with no LGE

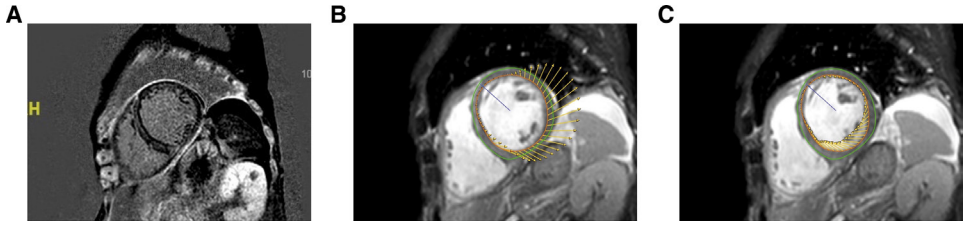

Figure 4 Late gadolinium enhancement (LGE) and myocardial deformation in a patient with dilated cardiomyopathy (DCM). LGE in a basal septal midwall linear pattern in DCM (A). Diastolic phase in DCM, impaired relaxation of LGE-positive myocardial segments (B). Systolic phase in DCM, impaired contraction of LGE-positive myocardial segments (C). Note, length of arrows displays relative extend of deformation.

or non-mid-wall LGE (p=0.801 and p=0.744, respectively). This finding could be explained by confounding effects of diffuse myocardial scarring that could have blurred effects of focal LGE. However, since the CMR protocol did not routinely include post-contrast T1 mapping, we could not assess ECV as additional marker for diffuse fibrosis to further evaluate this point. Diffuse fibrosis is thought to play an essential role in myocardial remodelling in DCM[33] and previous studies have detected the latter in DCM via T1 mapping.[33–35] Abnormalities in T1 relaxation times have been found already at early stages of the disease when changes in EF were only mild,[8] and were found to be associated with all-cause mortality.[36] In a CMR-FT analysis by Mazurkiewicz *et al*., LV circumferential strain rate and RV radial strain rate were independent predictors of large amounts of LV and RV fibrosis assessed by T1 mapping in 27 DCM patients.[37] Another study using CMR tagging found a significant correlation between the amount of fibrosis assessed by T1 mapping and circumferential strain in DCM patients,[38] while Chen *et al* could only show a weak correlation between T1 values and CMR-FT strain parameters in patients with severe DCM.[39]

Regional myocardial strain pattern

Mean LV_{SAX}-RS was most profoundly reduced in the basal septal segments II and III (figure 1). This reduction in strain was localised as LV_{SAX}-RS was preserved in the adjacent mid-ventricular septal segments, basal anterior and inferior as well as basal lateral segments (figure 1). LV_{SAX}-RS values were significantly lower in the basal septal segments compared with the other myocardial segments. LV_{SAX}-CS demonstrated a less distinct distribution pattern, but was overall higher in the lateral myocardial segments compared with the septum (figure 1). To our knowledge, an entity-specific strain pattern in DCM has not been described so far. One study using speckle tracking echocardiography (STE) reported higher apical regional LS and lower basal regional LS in non-ischaemic cardiomyopathy patients compared with ischaemic cardiomyopathy patients.[40] However, this study did not focus on DCM patients exclusively.

Association of regional myocardial strain and focal myocardial scar

Although there was a coincidence of impaired LV_{SAX}-RS and focal myocardial fibrosis in the basal septal myocardial segments, we did not find a significant effect of focal myocardial fibrosis on regional strain. This finding could be related to diffuse myocardial alterations, which were not detectable by LGE (table 2). Figure 4 illustrates the distribution of basal septal scarring and regional LV_{SAX}-RS in a patient of our study population. To the best of our knowledge, this is the first study to evaluate the relationship of focal myocardial fibrosis and segmental strain values in DCM. However, the subject has been studied in other entities, such as post-fontan single ventricle patients. Here, patients with myocardial fibrosis had decreased local CS determined by myocardial tagging analysis.[41] A study of CMR-FT in paediatric hypertrophic cardiomyopathy (HCM) patients showed lower regional strain in the septum with focal myocardial scar compared with the free wall without focal myocardial scar.[42] Another study in competitive athletes with normal LVEF showed reduced segmental RS in LGE-positive segments or in directly adjacent segments.[43] Additionally, a study using STE and comprising 30% of DCM patients within the study population reported that approximately 70% of LGE-positive segments had concomitant LS reduction.[44] Regional strain values, in particular, seem to be more useful than global strain values as fibrosis is often subtle and localised.

Limitations and future research

We acknowledge the following limitations: first, our study comprises a small sample size and does not address a possible prognostic value of the described strain patterns. Studies investigating a prognostic benefit have mainly focused on GLS and data concerning GCS and GRS are still scarce. Our results should therefore be confirmed in a larger cohort and a longitudinal study and extended to the assessment of a potential prognostic impact of strain patterns in DCM. Second, the technique of CMR-FT still needs further validation. While CMR-FT has shown good reproducibility for global strain values,[45] the reproducibility for segmental strain values seems to be limited.[7 46] Third, as the CMR protocol did not routinely include postcontrast MOLLI sequences, we could not assess ECV as marker for diffuse fibrosis next to LGE as marker for

focal fibrosis, which would have been useful to investigate the issue of more profoundly reduced LV_{SAX}-RS in the basal septal segments.

Additionally, it would be interesting to analyse strain patterns in DCM patients at early disease stages with only mild to moderate reduction in LVEF as GLS is thought to be an earlier disease marker in DCM compared with LVEF.[10 47]

One potential future clinical application could also be the assessment of borderline candidates for primary prophylactic ICD implantation. Considering studies such as the Danish Study to Assess the Efficacy of ICDs in Patients with Non-Ischemic Systolic Heart Failure on Mortality (DANISH),[48] risk stratification of these patients needs to be improved. In this regard, strain parameters could serve as additional risk predictors.

CONCLUSION

Our findings revealed a coincidence of impaired radial strain and focal myocardial fibrosis in the basal septal LV myocardial segments of patients with DCM. Regardless of this pattern, we did not find a general, significant effect of myocardial fibrosis on strain in our cohort. Future studies are required to assess the potential prognostic implications of myocardial strain patterns in addition to the assessment of myocardial fibrosis in patients with DCM.

Author affiliations
[1]Department of Cardiology, University Heart & Vascular Center, University Medical Center Hamburg-Eppendorf, Hamburg, Germany
[2]Department of Vascular Surgery, Albertinen Krankenhaus, Hamburg, Germany
[3]Deutsches Zentrum für Herz-Kreislauf-Forschung e.V. (German Center for Cardiovascular Research), Partner Site Hamburg/Kiel/Lübeck, Hamburg, Germany
[4]Institute of Medical Biometry and Epidemiology, University Medical Center Hamburg-Eppendorf, Hamburg, Germany
[5]Department of Cardiology and Angiology, Regio Clinics, Elmshorn, Germany
[6]Department of Diagnostic and Interventional Radiology, University Medical Center Hamburg-Eppendorf, Hamburg, Germany

Contributors Conceptualization: CC, EC, KM. Formal analysis: CC, KK, EC, KM. Statistical analysis: GS, CC. Guarantor: CC. Writing and editing: all authors.

Funding The authors have not declared a specific grant for this research from any funding agency in the public, commercial or not-for-profit sectors.

Competing interests None declared.

Patient consent for publication Not applicable.

Ethics approval The study was conducted in accordance with the principles of the Declaration of Helsinki and was approved by Hamburg Ethics Committee of the General Medical Council Hamburg (PV 4443). Participants gave informed consent to participate in the study before taking part.

Provenance and peer review Not commissioned; externally peer reviewed.

Data availability statement All data relevant to the study are included in the article or uploaded as supplementary information.

ORCID iDs
Céleste Chevalier http://orcid.org/0000-0002-3685-672X
Gerhard Schön http://orcid.org/0000-0003-2556-6804

REFERENCES

1 Maron BJ, Towbin JA, Thiene G, *et al*. Contemporary definitions and classification of the cardiomyopathies. *Circulation* 2006;113:1807–16.
2 Jefferies JL, Towbin JA. Dilated cardiomyopathy. *Lancet* 2010;375:752–62.
3 Pinto YM, Elliott PM, Arbustini E, *et al*. Proposal for a revised definition of dilated cardiomyopathy, hypokinetic non-dilated cardiomyopathy, and its implications for clinical practice: a position statement of the ESC working group on myocardial and pericardial diseases. *Eur Heart J* 2016;37:1850–8.
4 Adams KF, Dunlap SH, Sueta CA, *et al*. Relation between gender, etiology and survival in patients with symptomatic heart failure. *J Am Coll Cardiol* 1996;28:1781–8.
5 Messroghli DR, Moon JC, Ferreira VM, *et al*. Clinical recommendations for cardiovascular magnetic resonance mapping of T1, T2, T2* and extracellular volume: a consensus statement by the Society for Cardiovascular Magnetic Resonance (SCMR) endorsed by the European Association for Cardiovascular Imaging (EACVI). *J Cardiovasc Magn Reson* 2017;19:75.
6 Schulz-Menger J, Bluemke DA, Bremerich J, *et al*. Standardized image interpretation and post-processing in cardiovascular magnetic resonance - 2020 update. *J Cardiovasc Magn Reson* 2020;22:19.
7 Amzulescu MS, De Craene M, Langet H, *et al*. Myocardial strain imaging: review of general principles, validation, and sources of discrepancies. *Eur Heart J Cardiovasc Imaging* 2019;20:605–19.
8 aus dem Siepen F, Buss SJ, Messroghli D, *et al*. T1 mapping in dilated cardiomyopathy with cardiac magnetic resonance: quantification of diffuse myocardial fibrosis and comparison with endomyocardial biopsy. *Eur Heart J Cardiovasc Imaging* 2015;16:210–6.
9 Yu Y, Yu S, Tang X, *et al*. Evaluation of left ventricular strain in patients with dilated cardiomyopathy. *J Int Med Res* 2017;45:2092–100.
10 Romano S, Judd RM, Kim RJ, *et al*. Feature-tracking global longitudinal strain predicts death in a multicenter population of patients with ischemic and nonischemic dilated cardiomyopathy incremental to ejection fraction and late gadolinium enhancement. *JACC Cardiovasc Imaging* 2018;11:1419–29.
11 Claus P, Omar AMS, Pedrizzetti G, *et al*. Tissue tracking technology for assessing cardiac mechanics: principles, normal values, and clinical applications. *JACC Cardiovasc Imaging* 2015;8:1444–60.
12 Elliott P, Andersson B, Arbustini E, *et al*. Classification of the cardiomyopathies: a position statement from the European Society of Cardiology Working Group on Myocardial and Pericardial Diseases. *Eur Heart J* 2008;29:270–6.
13 Kawel-Boehm N, Hetzel SJ, Ambale-Venkatesh B, *et al*. Reference ranges ("normal values") for cardiovascular magnetic resonance (CMR) in adults and children: 2020 update. *J Cardiovasc Magn Reson* 2020;22:87.
14 Schulz-Menger J, Bluemke DA, Bremerich J, *et al*. Standardized image interpretation and post-processing in cardiovascular magnetic resonance - 2020 update: society for cardiovascular magnetic resonance (SCMR): board of trustees task force on standardized post-processing. *J Cardiovasc Magn Reson* 2020;22:19.
15 Selvadurai BSN, Puntmann VO, Bluemke DA, *et al*. Definition of left ventricular segments for cardiac magnetic resonance imaging. *JACC Cardiovasc Imaging* 2018;11:926–8.
16 Cavus E, Muellerleile K, Schellert S, *et al*. CMR feature tracking strain patterns and their association with circulating cardiac biomarkers in patients with hypertrophic cardiomyopathy. *Clin Res Cardiol* 2021;110:1757–69.
17 Scatteia A, Baritussio A, Bucciarelli-Ducci C. Strain imaging using cardiac magnetic resonance. *Heart Fail Rev* 2017;22:465–76.

18 Fox J, Weisberg S. *An R companion to applied regression*. Thousand Oaks: Sage Publishing, 2019.
19 Kuznetsova A, Bruun Brockhoff P, Bojesen Christensen RH. lmerTest: tests for random and fixed effects for linear mixed effect models (lmer objects of lme4 package), 2014. Available: http://r-forge.r-project.org/projects/lmertest/
20 Team. RC. R: a language and environment for statistical computing, 2022. Available: https://www.r-project.org/
21 Bland JM, Altman DG. Statistical methods for assessing agreement between two methods of clinical measurement. *Lancet* 1986;1:307–10.
22 Prasad SK, Tayal U. The value of strain in familial dilated cardiomyopathy screening. *JACC Cardiovasc Imaging* 2020;13:559–61.
23 Motoki H, Borowski AG, Shrestha K, *et al*. Incremental prognostic value of assessing left ventricular myocardial mechanics in patients with chronic systolic heart failure. *J Am Coll Cardiol* 2012;60:2074–81.
24 Buss SJ, Breuninger K, Lehrke S, *et al*. Assessment of myocardial deformation with cardiac magnetic resonance strain imaging improves risk stratification in patients with dilated cardiomyopathy. *Eur Heart J Cardiovasc Imaging* 2015;16:307–15.
25 Ochs A, Riffel J, Ochs MM, *et al*. Myocardial mechanics in dilated cardiomyopathy: prognostic value of left ventricular torsion and strain. *J Cardiovasc Magn Reson* 2021;23:136.
26 Francone M. Role of cardiac magnetic resonance in the evaluation of dilated cardiomyopathy: diagnostic contribution and prognostic significance. *ISRN Radiol* 2014;2014:1–16.
27 Assomull RG, Prasad SK, Lyne J, *et al*. Cardiovascular magnetic resonance, fibrosis, and prognosis in dilated cardiomyopathy. *J Am Coll Cardiol* 2006;48:1977–85.
28 Gulati A, Jabbour A, Ismail TF, *et al*. Association of fibrosis with mortality and sudden cardiac death in patients with nonischemic dilated cardiomyopathy. *JAMA* 2013;309:896–908.
29 Kuruvilla S, Adenaw N, Katwal AB, *et al*. Late gadolinium enhancement on cardiac magnetic resonance predicts adverse cardiovascular outcomes in nonischemic cardiomyopathy: a systematic review and meta-analysis. *Circ Cardiovasc Imaging* 2014;7:250–8.
30 Perazzolo Marra M, De Lazzari M, Zorzi A, *et al*. Impact of the presence and amount of myocardial fibrosis by cardiac magnetic resonance on arrhythmic outcome and sudden cardiac death in nonischemic dilated cardiomyopathy. *Heart Rhythm* 2014;11:856–63.
31 Csecs I, Pashakhanloo F, Paskavitz A, *et al*. Association between left ventricular mechanical deformation and myocardial fibrosis in nonischemic cardiomyopathy. *J Am Heart Assoc* 2020;9:e016797.
32 Taylor RJ, Umar F, Lin ELS, *et al*. Mechanical effects of left ventricular midwall fibrosis in non-ischemic cardiomyopathy. *J Cardiovasc Magn Reson* 2016;18:1):1.
33 Nakamori S, Dohi K, Ishida M, *et al*. Native T1 mapping and extracellular volume mapping for the assessment of diffuse myocardial fibrosis in dilated cardiomyopathy. *JACC Cardiovasc Imaging* 2018;11:48–59.
34 Dass S, Suttie JJ, Piechnik SK, *et al*. Myocardial tissue characterization using magnetic resonance noncontrast T1 mapping in hypertrophic and dilated cardiomyopathy. *Circ Cardiovasc Imaging* 2012;5:726–33.
35 Puntmann VO, Voigt T, Chen Z, *et al*. Native T1 mapping in differentiation of normal myocardium from diffuse disease in hypertrophic and dilated cardiomyopathy. *JACC Cardiovasc Imaging* 2013;6:475–84.
36 Puntmann VO, Carr-White G, Jabbour A, *et al*. T1-mapping and outcome in nonischemic cardiomyopathy: all-cause mortality and heart failure. *JACC Cardiovasc Imaging* 2016;9:40–50.
37 Mazurkiewicz Łukasz, Petryka J, Spiewak M, *et al*. Biventricular mechanics in prediction of severe myocardial fibrosis in patients with dilated cardiomyopathy: CMR study. *Eur J Radiol* 2017;91:71–81.
38 Jacquier A, Maurel B, Largueze J-B, *et al*. Potential value of T1 mapping in dilated cardiomyopathy and correlation with circumferential strain. *J Cardiovasc Magn Reson* 2013;15:P165.
39 Chen R, Wang J, Du Z, *et al*. The comparison of short-term prognostic value of T1 mapping with feature tracking by cardiovascular magnetic resonance in patients with severe dilated cardiomyopathy. *Int J Cardiovasc Imaging* 2019;35:171–8.
40 Zuo H, Zhang Y, Ma F, *et al*. Myocardial deformation pattern differs between ischemic and Non-ischemic dilated cardiomyopathy: the diagnostic value of longitudinal strains. *Ultrasound Med Biol* 2020;46:233–43.
41 Basu SK, Broderick PT, Cupps BP, *et al*. Myocardial fibrosis and ventricular strain indices in post-fontan single ventricle patients: cardiac Mr assessment and prognostic significance. *J Cardiovasc Magn Reson* 2013;15:O99–O.
42 Bogarapu S, Puchalski MD, Everitt MD, *et al*. Novel cardiac magnetic resonance feature tracking (CMR-FT) analysis for detection of myocardial fibrosis in pediatric hypertrophic cardiomyopathy. *Pediatr Cardiol* 2016;37:663–73.
43 Tahir E, Starekova J, Muellerleile K, *et al*. Impact of myocardial fibrosis on left ventricular function evaluated by feature-tracking myocardial strain cardiac magnetic resonance in competitive male triathletes with normal ejection fraction. *Circ J* 2019;83:1553–62.
44 Spartera M, Damascelli A, Mozes F, *et al*. Three-dimensional speckle tracking longitudinal strain is related to myocardial fibrosis determined by late-gadolinium enhancement. *Int J Cardiovasc Imaging* 2017;33:1351–60.
45 Maceira AM, Tuset-Sanchis L, López-Garrido M, *et al*. Feasibility and reproducibility of feature-tracking-based strain and strain rate measures of the left ventricle in different diseases and genders. *J Magn Reson Imaging* 2018;47:1415–25.
46 Morton G, Schuster A, Jogiya R, *et al*. Inter-study reproducibility of cardiovascular magnetic resonance myocardial feature tracking. *J Cardiovasc Magn Reson* 2012;14:43.
47 Verdonschot JAJ, Merken JJ, Brunner-La Rocca H-P, *et al*. Value of speckle tracking-based deformation analysis in screening relatives of patients with asymptomatic dilated cardiomyopathy. *JACC Cardiovasc Imaging* 2020;13:549–58.
48 Køber L, Thune JJ, Nielsen JC, *et al*. Defibrillator implantation in patients with nonischemic systolic heart failure. *N Engl J Med* 2016;375:1221–30.